In Situ PAC Study of InPt Exchanged Zeolites under Different Redox Conditions

José M. Ramallo-López,[†] Aníbal G. Bibiloni,[†] Félix G. Requejo,*[,†,‡] Laura B. Gutiérrez,[§] and Eduardo E. Miró[§]

Dpto. de Fisica, Fac. de Cs Exactas, UNLP e Instituto de Física de La Plata, CONICET, CC67−1900, La Plata, Argentina, and INCAPE (CONICET), Fac. Ingeniería Química, UNL, Santiago del Estero 2829, 3000 Santa Fe, Argentina

Received: November 8, 2001; In Final Form: May 17, 2002

The effect of reduction treatments in H_2 at 500 °C in both wet and dry atmosphere on mono and bimetallic In−zeolite supported catalysts has been studied using the perturbed angular correlation technique. The relaxation in the observed hyperfine interaction has been associated with the formation of oxygen vacancies in the indium sesquioxide particles present on the external surface of the catalysts. The addition of Pt has consequences for the relaxation process. The effect of Pt atoms could be associated with the trapping of vacancies, thus slowing down their jump frequency. This particular and indirect In−Pt interaction does not seem to have any effect on the enhancement of the catalytic activity observed in the bimetallic sample. A new indium species with cubic symmetry for the In site, i.e., metallic indium and/or In_2O_3 nanosized crystallites, was detected in reduced In/ferrierite and InPt/ferrierite samples.

Introduction

The use of perturbed angular correlations (PAC) in the characterization of species present in catalysts, and in particular their correlation with their catalytic activity, has led to interesting results which were unreachable by conventional techniques. This technique, through the measurement of the local electric field gradient (EFG) at a radioactive probe site, can give information about the characteristics (coordination, symmetry, distortions, etc.) of the different environments of the radioactive probes, their concentrations and modifications related to in situ conditions, i.e., reaction temperatures and high pressures with different reactant gases. This is possible by means of the hyperfine interaction between the nucleus of the radioactive probe and the EFG produced by the extranuclear (ion and electronic) charges.[1] The sensitivity of the PAC technique is independent of the temperature or the pressure on the sample and also allows the detecting of different phases in the sample. On the other hand, because the information is extracted from relatively high-energy gamma rays (typically hundreds of keV), it is possible to use nearly any reaction vessel. A detailed explanation of the technique can be found elsewhere.[2,3]

Inspired by the pioneering work of Butz et al. [4] our group has successfully applied this technique to the study of Mo supported systems [5−7] and more recently to indium containing catalysts.[8,9] In the first case, we could identify the molybdenum species present on the surface of oxide supports (SiO_2, Al_2O_3, and TiO_2/Al_2O_3) complementing the PAC results with conventional spectroscopy studies. In indium−zeolite systems, we could characterize and quantify the active site for the selective catalytic reduction (SCR) of NO with CH_4 and study their formation on different zeolites (like ZSM5 and Ferrerite) and under different methods of preparation. However, some aspects of the characteristics of these species and their interaction with hydrogen during activation treatments are still open.

Because of its capacity to make in situ characterizations with the sample in a reactor and under a gas flux and its sensitivity to detect the presence of very dispersed, diluted species not seen with conventional techniques, PAC is suitable to study the effect of different gas fluxes on the species present in the catalysts without any modification of the usual reaction conditions. In this respect, the study of the effect of H_2 and water vapor on indium species and their possible interaction with metallic promoters using the PAC technique should indicate a different characteristic for In active sites. In effect, in the case of the bimetallic InPt/ferrierite zeolite, we found that the reduction process in H_2 constitutes an activation method for the catalyst,[10] whereas the activity after reduction is practically null for the monometallic In/FER catalysts. The effect of promoters as Pt in metallic catalysts has been extensively studied,[11−13] and the appearance of alloys or other bimetallic entities has been the common explanation of such effects. We have already studied these catalysts before and after reduction by means of Pt L_3 EXAFS, and no signs of interaction between indium and platinum were found.[10] The present PAC study has interest not only in the determination of the interaction of the indium with hydrogen but also in understanding this activation effect by reduction. In particular, the study of the catalyst during in situ reduction in H_2 is expected to give some insight to this yet unexplained behavior. Furthermore, the interaction of indium with H_2O is of great interest in catalysis because it has been shown that it may have both promotional[9] and retardation effects[14] on the catalytic activity of In/zeolite systems. As a consequence, it is necessary to understand the evolution of indium species under these in situ conditions in order to explain this interesting behavior. To shed new light on this issue, PAC measurements were performed on In/FER, InPt/FER, and In/ZSM5 catalysts under air, hydrogen, and hydrogen with different pressures of water vapor using the radioactive $^{111}In \rightarrow {}^{111}Cd$

* To whom correspondence should be addressed. E-mail: requejo@stm.lbl.gov.

† Dpto. de Física, Fac. de Cs. Exactas, UNLP e Instituto de Física de La Plata (CONICET).

‡ Present address: Materials Science Division, LBNL, Mailstop 66-200, Berkeley, CA 94720. Phone: (510) 486-4213. Fax: (510) 486-4995.

§ INCAPE (CONICET), Fac. Ingeniería Química, UNL.

10.1021/jp014098v CCC: $22.00
Published on Web 07/18/2002

PAC probe. Experiments were carried out in order to compare the effect of the Pt addition and the zeolitic support on the evolution of the species through the different treatments.

Experimental Section

In/FER was prepared by the standard ionic exchange method, stirring an aqueous solution of $InCl_3$ (0.003 M) and FER at 80 °C (with reflux) during 24 h, followed by filtering and distilled-water washing. After that, the sample was dried in a stove at 120 °C and calcined in air at 500 °C during 12 h. In this way, an In-exchanged sample with 0.5 wt % of In was obtained. InPt/FER was obtained in the same way, using Pt/FER as the starting material.

In/ZSM5 was prepared by the conventional wet impregnation method, stirring an aqueous solution of $InCl_3$ and NH_4-ZSM5 at 80 °C until all water was evaporated, followed by drying in a stove at 120 °C during 12 h. A certain amount of $InCl_3$ was added in order to obtain a sample with 4 wt % of In. After that, the solid was pretreated by heating in air up to 500 °C at 5 °C/min and holding the final temperature for 12 h. Finally, the sample was calcined for 2 h in air at 750 °C. This sample was used to study the effect of the support and the In concentration on the interaction of indium species with H_2.

To perform the PAC experiments, the ^{111}In probe was introduced by adding traces of $^{111}InCl_3$ to the nonradioactive $InCl_3$ solution.

The primary physical quantity accessible in a PAC experiment is the electric field gradient tensor acting on the probe nucleus. The electric field gradient V_{ij} is the second spatial derivative of the electric potential, and it is a traceless second rank tensor quantity, which is conventionally described in its principal axes system by its largest diagonal element V_{zz} and an asymmetry parameter $\eta = (V_{yy} - V_{xx})/V_{zz}$, describing the symmetry of the tensor about its z-principal axis ($\eta = 0$ corresponding to axial symmetry in this notation). It has been shown both by experiment [15] and theory [16] that V_{zz}, η, and the orientation of the principal axes system are highly sensitive to the local charge distribution around the probe nucleus thus revealing distinct information on the site occupied by the probe atom.

In this work, a four BaF-detector fast−fast coincidence system in a coplanar arrangement was used to perform the PAC experiments. The crystals of the detector units had the shape of truncated-cone-capped cylinders, with a 44 mm diameter base, 30 mm in height, a 20 mm diameter at the top, and a conical angle of 90°. The face in contact with the photomultiplier was optically polished (in order to achieve a good transmission of the ultraviolet photons from the crystal to the photomultiplier tube), whereas the remaining surfaces were opaque. The geometry of the crystals was conceived in order to be able to locate the detectors at a distance of about 20 mm from the sample and to detect in efficient form γ-rays of up to 1 MeV. It has also been demonstrated that the use of conical scintillators improved the temporary response of the detectors, because the time of collection of light in the crystals is minimized.[17] The energy resolution of this unit is 9.5% for γ-rays of 662 keV, which is enough to resolve γ_1 and γ_2 of the more usual PAC probes, and the time resolution of the spectrometer is 0.8 ns (full width at half-maximum of the prompt peak).

Eight coincidence spectra (four at 90° and four at 180°) of all possible start−stop combinations of the four detectors were simultaneously recorded in a multichannel analyzer. A coincidence $C_{ij}(t)$ is the result of the detection of the two γ-rays from a cascade decay coming from the same nucleus in detectors i and j separated an angle of $\theta°$ with an interval of t seconds between them. From the coincidences at two angles (90° and 180°) these two relations can be constructed:

$$W(180°, t) = [C_{13}(t) + C_{31}(t)]^{1/2}\,[C_{24}(t) + C_{42}(t)]^{1/2} \quad (1)$$

and

$$W(90°, t) = [C_{12}(t) + C_{21}(t)]^{1/2}\,[C_{34}(t) + C_{43}(t)]^{1/2} \quad (2)$$

Finally, the asymmetry ratio $R(t)$ becomes

$$R(t) = 2\frac{[W(180°, t) - W(90°, t)]}{W(180°, t) + 2W(90°, t)} \approx A_{22}^{\exp}\, G_{22}(t) \quad (3)$$

with $A_{22}^{\exp}$ being the effective anisotropy of the cascade for a certain experimental condition and $G_{22}(t)$ the perturbation factor containing the relevant information about the hyperfine interaction.

If the perturbation is caused by a static EFG acting on the probe nucleus of quadrupole moment Q and the EFG tensor is described by its main component V_{zz} and the asymmetry parameter η, the perturbation factor is

$$G_{22}(t) = \sum_i f_i (S_{20,\,i} + \sum_{n=1}^{3} S_2 n,i \cos(\omega_{ni} t) e^{-\delta_i \omega_{ni} t}) \quad (4)$$

The ω_n frequencies are related to the quadrupole frequency $\omega_Q = eQV_{zz}/40\hbar$, by the relation $\omega_n = g_n(\eta)$. The g_n and S_{2n} coefficients are known functions[18] of the asymmetry parameter η. The exponential functions in eq 4 account for a Lorentzian frequency distribution of relative width δ around ω_n and give information about the homogeneity of the site associated to that interaction. Theoretical functions of the form $A_{22}^{\exp}\, G_{22}(t)$ with $G_{22}(t)$ defined like in eq 4 were fitted to the experimental $R(t)$ anisotropy ratio. In this way, the hyperfine parameters for each of the relative fractions of nuclei that experience a given perturbation f_i are determined. The number of the n different f_i (with $i = 1, ..., n$) used to fit the spectra is equal to the different sites the probe nucleus occupies.

Besides the static EFG, time dependent relaxation processes may sometimes be observed in PAC measurements giving rise to a specific $G_{22}(t)$. Different causes can be the origin of such behavior. In the case of the ^{111}In probe, the so-called "after effects" following the nuclear electron capture decay of the probe should always be considered. This perturbation is ultimately produced by a hole trapped in the impurity center introduced by the ^{111}Cd decay in the band gap of the semiconductor.[19] Two different electron−hole recombination mechanisms were identified: electrons coming from the conduction band mostly dominate the recombination process at low temperature (from −259 to −73 °C), whereas the thermal excitation of electrons from the valence band is the most important source of electron supply at higher temperatures.[20] For the case of In_2O_3, practically no attenuation is observed above 350 °C.[19] Liquid phases can also lead to the appearance of relaxation processes.[21] In liquid metals and alloys, time-dependent relaxation is due to fluctuating electrical field gradients. It is well established that the main contribution to these fluctuations comes from the thermal motion of the ions surrounding a probe atom. Four different relaxation processes may be distinguished: hard collisions, diffusion, decay of associates, and rotational diffusion. However, it has been reported that in the case of ^{111}In in liquid In metal a random fluctuation takes place which averages the interaction to zero.[22] No precession takes place in such a zero field and only the

unperturbed term ($S_0 = 0$, $\omega_Q = 0$) remains in the PAC spectrum. A third time-dependent type of interaction occurs when the environment of the probe changes rapidly. This situation can occur when rapidly moving defects such as vacancies contribute significantly to the hyperfine fields experienced by the probe nucleus.[23] In this latter case, two models are known:[24] (a) the Marshall−Meares model which corresponds to the slow relaxation limit in which the perturbation factor can be written as the static perturbation factor multiplied by an attenuation factor of the form $e^{\lambda t}$ [25] and (b) the Abragam and Pound model which corresponds to the fast relaxation limit in which the perturbation factor results in a pure exponential decay of the anisotropy of the form $e^{-\lambda t}$.[26] The relaxation constant λ is related to the jump frequency of the vacancies.[27] On the basis of Blume's stochastic theory of PAC [28] and the model developed by Winkler and Gerdau,[29] Evenson et al.[30] proposed a more realistic model in which several different exponentials contribute to the damping. However, the authors agree that, in many practical situations, the simplest approximation may be adequate. In our case, the spectra showing relaxation were fitted using the Abragam and Pound model to determine the relaxation constant. Practically, this is done by fitting the $Ae^{-\lambda t} + F_0$ function to the spectra. In this case, A is the anisotropy, λ is the relaxation parameter, and F_0 is the proportion of probes experiencing a cubic EFG.

All PAC measurements were performed at 500 °C because this is the temperature at which these catalysts show their higher conversion of NO,[8,9] so the species-characterization becomes interesting at this temperature. Moreover, it has been reported that the so-called after-effects are completely removed at this temperature, at least for indium sesquioxide.[19] These after-effects can produce an attenuation of the spectra and may make the analysis more difficult. The PAC measurements were performed after preparation in air. Temperatures higher than 500 °C were not used in order to avoid possible break-down of the ferrierite structure or zeolite dealumination,[31] which would result in a change of In's local environment. It should be said that in order to make a quantitative and reliable determination of the relaxation constant, a temperature dependent determination is required. However, because of the limitations already mentioned regarding measurements at different temperatures, we have only measured at one temperature. Because of this limitation, we should take into account the fact of the existence of a relaxation process at some temperature and its qualitative aspects, rather than any quantitative speculation about the process.

The samples were then reduced in H_2 flux (AGA high purity, 99.999%) during 2 h to complete the reduction process and to perform the PAC measurement on a static state if one is reached. Finally, samples were reoxidized in air during 1 h and measured in those conditions. Some samples were also measured in a combined flux of H_2 and vapor H_2O at different pressures. Feed gas mixtures of about 2 mol % and 15 mol % H_2O/H_2 were prepared by flowing H_2 through a distilled water saturator held at 20 °C and 55 °C, respectively.

Results

The PAC spectra measured at 500 °C for In/FER catalyst in air, in H_2 flux, and in air again after reoxidation as well as the fitted $R(t)$ function and their Fourier transforms are shown in Figure 1 parts a−c, respectively. The spectra show great changes in the species of indium present in each step of the process, indicating that the reduction treatment has an important effect on the catalyst. The hyperfine parameters fitted for the three spectra are detailed in Table 1. As we have previously

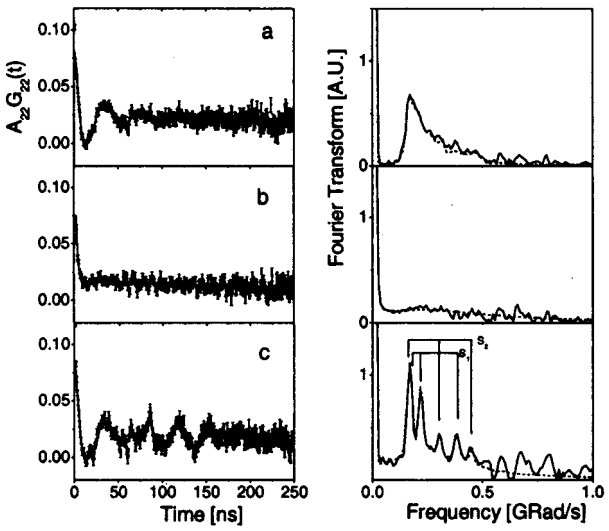

Figure 1. Left: PAC spectra of In/FER measured at 500 °C in air (a), in H_2 (b), and in air after reoxidation (c). Solid lines show the least-squares fit to the data. Right: their corresponding Fourier transforms. Solid line: experimental data. Dashed line: fit.

reported,[8,32] three sites for indium are found after preparation. The first two (S_1 and S_2) correspond to the two nonequivalent lattice sites of indium in bulk In_2O_3.[33] Thus, 70% of indium atoms in the catalyst are forming bulk indium sesquioxide. Differences compared to the pure In_2O_3 case should be associated with the small dimensions of the crystallites present in the catalysts. In particular, the distributions of both sites are larger than those found for bulk indium sesquioxide, and the relation of their population is not 3 to 1 as found in bulk oxide. It should be noted that X-ray diffraction (not presented in this work) does not show the presence of such oxides indicating that the crystallite sizes are below the resolution of this technique, i.e., <5 nm. The third site S_3 has been previously assigned to $(InO)^+$ at the cationic exchange sites of the zeolite and constitutes the active sites for the selective catalytic reduction (SCR) of NO.[8,9]

During the reduction treatment, all characteristic signals of indium sesquioxide disappear (Figure 1.b) and a relaxation is necessary to fit the spectrum. We have used the Abragam and Pound model fitting an $e^{-\lambda t}$ function to determine the relaxation constant (Table 1), which indicates a time dependence of the configuration of the In surrounding. A baseline is also present making the hardcore different from zero and resulting in 20% of f_0, which accounts for the percentage of probes experiencing a zero EFG. Although a distribution could also be responsible for this baseline, we have chosen to use an f_0 to fit it for reasons that will be explained later. After the reoxidation (Figure 1c), three sites are found again as in the catalyst after preparation. Both characteristic signals of sites of indium in In_2O_3 are present again, but in a smaller quantity and better defined than in the original sample (their distributions δ are smaller and their population relation is now 3 to 1). However, hyperfine parameters corresponding to $(InO)^+$ species at cationic exchange sites of the zeolite are not present, and a new one is found (S_5).

The InPt/FER catalyst has a similar PAC spectrum as In/FER after calcination as we have already reported (Figure 2a and Table 2).[32] During reduction (Figure 2b), a relaxation is also observed, but the time constant is different from that of the monometallic catalyst. A baseline is also present and, as in the In/FER catalyst, 20% of probes experience a null EFG. After reoxidation (Figure 2c), hyperfine parameters for three sites are found again as in the same catalyst after preparation. Both sites

TABLE 1: Fitted Values of the Parameters Characterizing the Observed Interactions in the In/FER PAC Spectra of Figure 1[a]

condition	population f [%]	frequency ω_Q [MHz]	asymmetry parameter η	distribution δ [%]	relaxation constant λ [ns^{-1}]	site
air	40(6)	118(2)	0.68(2)	6(2)		S_1
	35(6)	162(2)	0.41(3)	7(2)		S_2
	25(7)	222(2)	0.40(2)	7(2)		S_3
H_2[b]					0.0010(5)	S_R
air	33(4)	121(3)	0.71(2)	1.7(4)		S_1
	11(2)	157(3)	0.05(3)	1.0(7)		S_2
	56(5)	136(9)	0.6(2)	40(8)		S_5
bulk In_2O_3	74(3)	114(3)	0.74(1)	4(1)		S_1
[26]	20(2)	153(3)	0.22(2)	1(1)		S_2

[a] The hyperfine parameters reported in ref 26 for bulk In_2O_3 are included for comparison. All measurements were performed at 500° C. [b] A 20% of f_0 is present.

TABLE 2: Fitted Values of the Parameters Characterizing the Observed Interactions in the InPt/FER PAC Spectra of Figure 2[a]

condition	population f [%]	frequency ω_Q [MHz]	asymmetry parameter η	distribution δ [%]	relaxation constant λ [ns^{-1}]	site
air	45(7)	123(4)	0.71(2)	10(1)		S_1
	28(7)	157(4)	0.24(2)	5(1)		S_2
	27(7)	188(4)	0.32(3)	10(3)		S_3
H_2[a]					0.007(1)	S_R
air	36(5)	122(1)	0.71(2)	4(1)		S_1
	8(1)	157(2)	0.16(4)	1(1)		S_2
	56(3)	184(10)	0.7(3)	35(8)		S_3

[a] All measurements were performed at 500° C. [b] A 20% of f_0 is present.

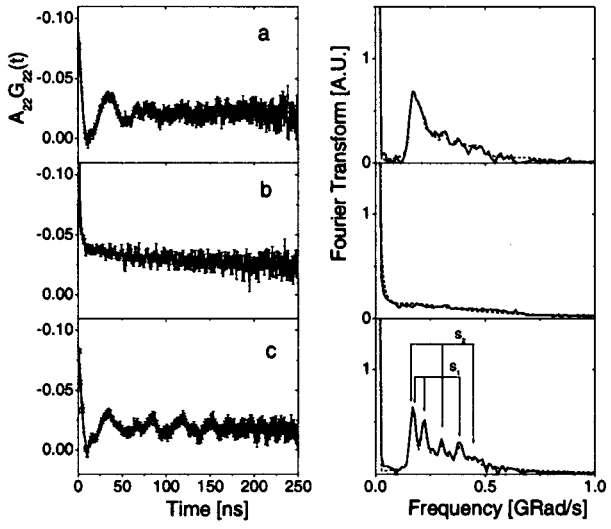

Figure 2. Left: PAC spectra of InPt/FER measured at 500 °C in air (a), in H_2 (b), and in air after reoxidation (c). Solid lines show the least-squares fit to the data. Right: their corresponding Fourier transforms. Solid line: experimental data. Dashed line: fit.

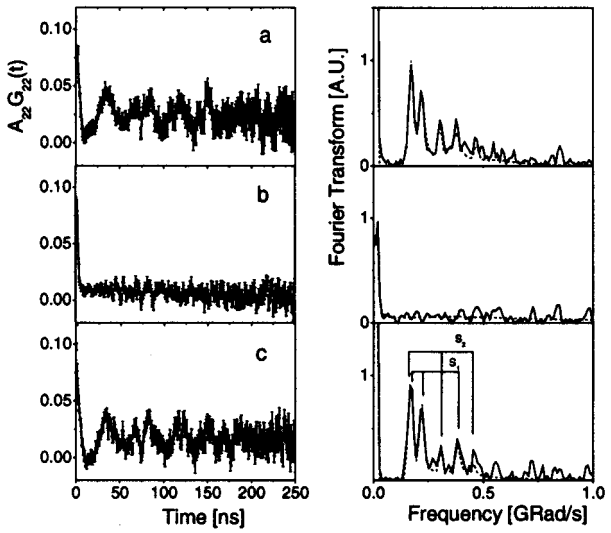

Figure 3. Left: PAC spectra of In/ZSM5 measured at 500 °C in air (a), in H_2 (b), and in air after reoxidation (c). Solid lines show the least-squares fit to the data. Right: their corresponding Fourier transforms. Solid line: experimental data. Dashed line: fit.

of indium in In_2O_3 are present, but their amounts are smaller than in the first spectrum. The frequency distributions around the mean values are smaller, and the population ratio between sites is 3:1, in agreement with their crystallographic abundance. The hyperfine parameters corresponding to the $(InO)^+$ at cationic exchange sites of the zeolite appears now in a higher concentration (56%).

Figure 3 shows the same set of measurements for In/ZSM5 catalysts. A similar trend as the one described above for the InPt/FER catalyst is observed. Three hyperfine interactions are fitted for the catalyst in air indicating the presence of In_2O_3 and $(InO)^+$ at the cationic exchange sites of the zeolite (Table 3). The hyperfine interactions corresponding to the two sites for indium in In_2O_3 are better defined than in the previous samples (their frequency distributions are smaller), indicating the presence of larger crystals. During reductive conditions, both species disappear and a relaxation is again observed, similar to that found for In/FER. However, there is no baseline as in FER based catalysts, indicating that there are no nuclei with zero EFG present. After reoxidation, In_2O_3 and $(InO)^+$ reappeared in the same proportions as they were found before reduction.

PAC measurements under a combined flux of H_2 and water vapor are shown in Figures 4 and 5. The first spectra correspond to the as-prepared catalyst, and the species found are the same as those described above, showing that the starting materials are the same. When water is added to the H_2 feed, a change in the spectra for the InPt/FER catalyst is observed (Figure 4 parts b and c), and besides the relaxation, a static perturbation appears. The fitted parameters show that this interaction is better defined (i.e., with a minor value for distribution δ) as the quantity of water vapor is increased (Table 4). In adittion, no baseline is present. In contrast, no such effect is observed in the In/ZSM5

TABLE 3: Fitted Values of the Parameters Characterizing the Observed Interactions in the In/ZSM5 PAC Spectra of Figure 3[a]

condition	population f [%]	frequency ω_Q [MHz]	asymmetry parameter η	distribution δ [%]	relaxation constant λ [ns^{-1}]	site
air	37(4)	120(6)	0.67(1)	3.3(5)		S_1
	17(3)	159(6)	0.33(2)	0.7(4)		S_2
	46(4)	193(20)	0.35(5)	15(5)		S_3
H_2					0.0010(5)	S_R
air	47(6)	121(6)	0.7(1)	2.5(5)		S_1
	12	158(6)	0.05(5)	0.6		S_2
	41	178(24)	0.6(3)	49(4)		S_3

[a] All measurements were performed at 500° C.

TABLE 4: Fitted Values of the Parameters Characterizing the Observed Interactions in the InPt/FER PAC Spectra of Figure 4[a]

condition	population f [%]	frequency ω_Q [MHz]	asymmetry parameter η	distribution δ [%]	relaxation constant λ [ns^{-1}]	site
air	46(6)	124(2)	0.66(3)	7(2)		S_1
	27(6)	151(2)	0.24(3)	4(1)		S_2
	27(6)	177(6)	0.35(2)	12(3)		S_3
2% H_2O+H_2	10(3)	120(5)	0.70(3)	5(1)		S_1
					0.010(3)	S_R
15% H_2O+H_2	15(3)	119(3)	0.67(3)	4(1)		S_1
	5(2)	159(3)	0.3(1)	1.0(6)		S_2
					0.019(3)	S_R
air	27(3)	121(5)	0.70(1)	0.8(4)		S_1
	10(4)	158(10)	0.11(2)	0.5(5)		S_2
	63(3)	180(6)	0.30(4)	26(2)		S_3

[a] All measurements were performed at 500° C.

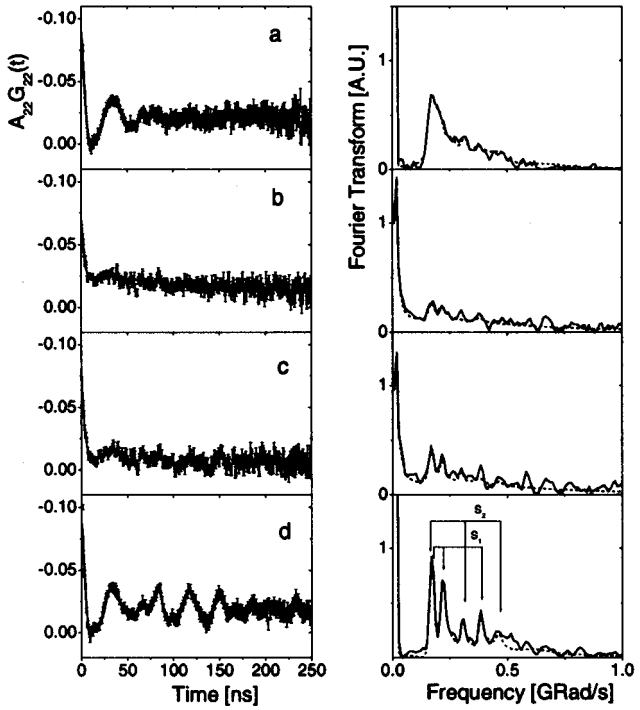

Figure 4. Left: PAC spectra of InPt/FER measured at 500 °C in air (a), in 2% H_2O + H_2 flux (b), and in 15% H_2O + H_2 flux (c). Solid lines show the least-squares fit to the data. Right: their corresponding Fourier transforms. Solid line: experimental data. Dashed line: fit.

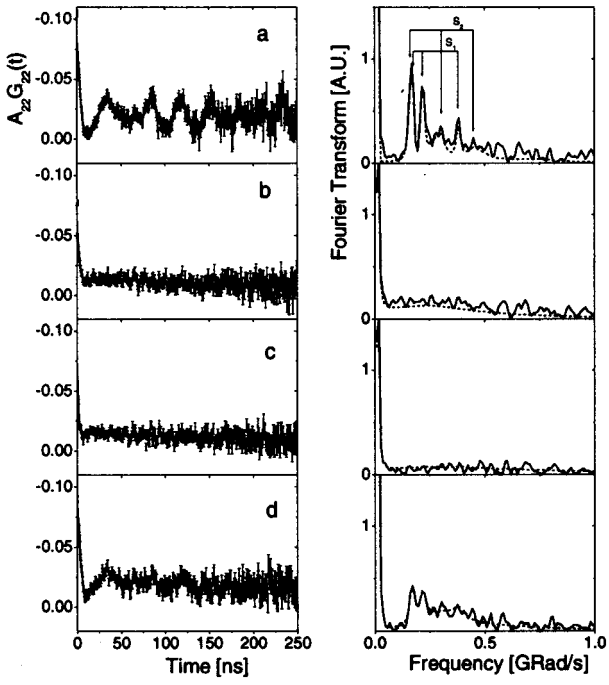

Figure 5. Left: PAC spectra of In/ZSM5 measured at 500 °C in air (a), in 2% H_2O + H_2 flux (b), in 15% H_2O + H_2 flux (c), and in air after reoxidation (d). Solid lines show the least-squares fit to the data. Right: their corresponding Fourier transforms. Solid line: experimental data. Dashed line: fit.

catalyst (Figure 5 and Table 5). In this case, when water vapor is added to the feed, no significant changes are observed in the relaxation.

After reoxidation, three sites for indium are found in both catalysts again, corresponding to In_2O_3 and $(InO)^+$ species. In the case of InPt/Fer, the populations are similar to those after reduction without water vapor, but their distribution is smaller, with both species being better defined. In the case of In/ZSM5, the quantity of In_2O_3 is smaller, and according to the catalytic test previously performed, more active sites appear.

Discussion

In previous works, we have already discussed the species present in the catalysts after calcination.[8−10,32] The most interesting results appeared during the reduction in H_2 at 500 °C. According to the literature,[34−36] treatments in H_2 at

TABLE 5: Fitted Values of the Parameters Characterizing the Observed Interactions in the In/ZSM5 PAC Spectra of Figure 5. All Measurements Were Performed at 500° C

condition	population f [%]	frequency ω_Q [MHz]	asymmetry parameter η	distribution δ [%]	relaxation constant λ [ns^{-1}]	site
air	37(4)	18.9(1)	0.67(1)	3.3(5)		S_1
	17(3)	25.0(1)	0.33(2)	0.7(4)		S_2
	46(4)	30.4(9)	0.35(5)	15(5)		S_3
2% H_2O+H_2					0.0010(5)	S_R
15% H_2O+H_2					0.0010(5)	S_R
air	20(7)	122(3)	0.66(2)	4(1)		S_1
	7(2)	164(6)	0.5(1)	3(1)		S_2
	73(4)	197(2)	1.0	50(6)		S_3'

500 °C favor the following reactions:

$$In_2O_3 + 2H_2 \rightarrow In_2O + 2H_2O \quad (5)$$

and

$$In_2O + H_2 \rightarrow 2In^0 + H_2O \quad (6)$$

$(InO)^+$ active sites are also easily reduced during this treatment following this reaction:

$$(InO)^+ + H_2 \rightarrow In^+Z^- + H_2O \quad (7)$$

where Z^- stands for the acid site of the zeolite. Under more severe reduction conditions, the In^+Z^- could also be reduced to give In^0. In this way, all In species present in the catalyst may end up as In^0. If this were the case, and considering the temperature during the PAC experiments and the indium melting point (156.6 °C), all indium atoms should be in the liquid state during reduction in H_2. It has already been reported[22] that for ^{111}Cd in liquid indium a rapidly enough random fluctuation of the EFG at the probe site takes place so that it causes the averaging out of it to null. No precession takes place in such a zero field and only the unperturbed term (characterized by $S_0 = 0$ and $\omega_Q = 0$) remains in the PAC spectrum. This is not the case of the spectra of the different samples in H_2 flux. In all of them, a time dependent EFG is present, and in the FER-based catalyst, it is superimposed to a percentage of probes experiencing a zero EFG, which in both cases is around 20%. This percentage constitutes a baseline in the PAC spectra and corresponds to $^{111}In \rightarrow {}^{111}Cd$ probes in cubic symmetry, like indium in liquid state or metallic indium at nanosized dimension. In effect, it was already reported that metallic nanoclusters of In exhibit cubic symmetry.[37,89] Another possible explanation for the origin of the EFG = 0 in In species can be associated with the presence of nanosized In_2O_3 crystallites. In recent scientific contributions, it has been shown that In_2O_3 nanowires[39] and nanoclusters[40] present a cubic symmetry for In sites. In our particular case, these nanosized In_2O_3 crystallites could be produced by the incomplete reduction of larger crystals. Furthermore, although a distribution could be fitted to account for this baseline, its disappearance when water is added to the feed makes us think it is due to a zero EFG.

As said before, in previous works,[9,10] we have characterized In/FER and InPt/FER, by means of temperature programmed reduction (TPR) and catalytic activity measurements during the SCR of NO_x with methane. We found that important changes in the distribution of the In species take place after reduction and reoxidation at 500 °C. The existence of liquid indium as a mobile phase during the reduction process is in agreement with the possibility of the formation of the active sites $(InO)^+$ from small indium sesquioxide crystals in the InPt/FER, increasing the catalytic activity and shifting the TPR peaks to lower temperatures. Because the mentioned transformation implies the migration of In atoms from the In sesquioxide crystals to the vicinity of the zeolite exchange sites, it would be difficult to understand how those transformations could readily take place without the existence of a mobile phase, such as liquid In.

No cubic phase is present in In/ZSM5 in H_2 or in InPt/FER when water is added to the H_2 feed. In the former case, the indium sesquioxide crystals are bigger than those found in In/FER and in InPt/FER, which is evident from their hyperfine parameters being closer to those of bulk indium sesquioxide. This makes the total reduction of the crystals following the reaction described above harder than in the case of FER catalysts, and no metallic indium phase is produced. The reason for the absence of metallic indium in the liquid phase in InPt/FER when water is added to the H_2 flux may be that the oxygen provided by the water molecules permits the oxidation of these metallic particles. This is evident from the appearance of indium sesquioxide as the main In species in these spectra and its increase in population with the amount of water. The more symmetric indium site cannot be fitted in the first spectrum because of its small population.

The most intriguing and interesting aspect of this study is the difference observed during reduction treatment between the mono- and the bimetallic catalyst. In the case of the two monometallic samples (In/FER an In/ZSM5), their spectra differ only in the baseline that is present in the first one, and this has already been discussed. As we have previously noted, we have already investigated the interaction between indium and platinum atoms in InPt/FER by means of Pt L_3-edge EXAFS experiments, but no evidence of bimetallic entities has been found. This made us assume that there was no interaction between both types of atoms, neither before nor after reduction treatments, and that the promotional effect of Pt on the SCR of NO was associated with the acceleration of one step of the reaction related with the appearance of metallic Pt nanoparticles.[10] We also reported an increase in the number of indium atoms at cationic exchange sites after reduction but could not relate this to the presence of Pt atoms.

During the reduction treatment, a relaxation is present in all catalysts with a different relaxation parameter λ for the mono and bimetallic ones. Before any analysis of the reasons for this behavior and the relation of this fitting parameter with a physical property of the systems, one important conclusion can be arrived at, and it is that indium probes are somehow influenced by the presence of Pt atoms in InPt/FER. The presence of Pt atoms is the only difference between both experiments and the only way to explain the difference in the relaxation process observed for this catalyst with respect to the monometallic ones. This constitutes the first evidence of an In−Pt interaction in our catalyst.

As we have said before, three reasons may be ascribed to the appearance of a relaxation in a PAC spectrum: after-effects,

TABLE 6: V_{ZZ} and η Values for In at C and D Sites of In_2O_3 with a Pt^{4+} Atom at Different First Neighbors Positions Calculated using the Point Charge Model[a]

Pt at site:	distance to site C [Å]	V_{zz} for site C [x10^{-21} V/m^2]	η for site C	distance to site D[Å]	V_{zz} for site D [x10^{-21} V/m^2]	η for site D
		−0.16115	0.82719		0.2497	0
C	3.36	0.15441	0.975	6.06	0.2395	0.011
C	3.83	−0.1357	0.439	3.82	0.22789	0.13
D	3.3478	−0.1777	0.8966	5.058	0.25034	0.091

[a] The first row shows the values obtained for pure In_2O_3.

liquid phases, and rapidly changing environments around the probe. We have discarded the first one because no evidence of after-effects for indium compounds has been reported at this temperature. The existence of liquid phases as the reason for the relaxation has to be discarded as well. It might be possible to explain this behavior for the bimetallic catalyst in terms of an In−Pt melt (not observed in a previous experiment by EXAFS [10]). In this case, the EFG produced by them could differ enough so that the cancellation of the two- and three-particle correlation functions is no longer perfect and the ions have to move longer distances to destroy the memory of the EFG at the probe and a relaxation process would occur.[30,41] However, this explanation would not be possible for the monometallic catalyst. The presence of liquid metallic indium in this catalyst, given the characteristics indicated above, could not bring about the observed relaxation. So, a rapidly changing environment around the probe site seems to be the only reasonable explanation of the observed effect. In our particular case, an oxygen vacancy that may be free to jump between equivalent near-neighbor positions seems to be the reason for the relaxation process. Such effects have already been reported when using ^{111}In PAC spectroscopy to study trapping and hopping of oxygen vacancies near indium and its daughter isotope, cadmium, in a variety of zirconia-based ceramics,[42,43] and ceria oxide [44] as well as for ^{181}Hf PAC spectroscopy studies of defect dynamics in pure CeO_2.[45] The reducing atmosphere of H_2 would be responsible for the creation of such oxygen vacancies.

To discuss the difference we found in the values of the parameter λ for the mono and bimetallic catalysts, we may imagine the following scenario. During reduction either with H_2 or with $H_2 + H_2O$, oxygen vacancies are created in the indium sesquioxide crystallites. This is consistent because it is known that indium sesquioxide is an n-type semiconductor. Let us assume that several percents of oxygen vacancies are created by reduction. Because of charge considerations, Cd impurities should be attractive traps for oxygen vacancies. Thus, vacancies should be at first-neighbor positions for Cd. In this way, almost all Cd cations should be associated to at least one oxygen vacancy because cadmium impurities are only present at trace level in this compound.

We will discuss first the case of the monometallic catalysts after reduction. At 500 °C vacancies should be mobile and able to jump among equivalent trap sites. Pryde et al. [46] have shown that in the case of ceria the jump of oxygen vacancies at temperatures as low as 200 °C was enough to justify the nonstatic hyperfine interaction revealed by the PAC spectra. In addition, they calculated these interactions obtaining results very close to those found by PAC. In a very simple model, assuming that the vacancies jump over an energy barrier of 0.6−0.8 eV which is the case of ceria, and a characteristic frequency $\nu_0 = 10^{13}$ 1/s, we obtained for 500 °C, $\nu = 1.2 \times 10^{-4}$ to 6×10^{-4} 1/ns. These jump frequencies that imply changes in the EFG orientation as the oxygen vacancy changes its crystalline position are fast enough to produce a loss in the memory of the spin orientation, i.e., a time dependent relaxation process.

According to Baudry and Boyer,[27] the relaxation parameter λ is related to the jump frequency through $\lambda = (N - 1)\nu$ or through $\lambda = 100\ \omega_Q 2/N\nu$ depending on condition $\nu < \omega_Q$ and $\nu > 20\omega_Q$, respectively. Here, N is the number of first neighbors, which in our case is 6. To estimate the value of ω_Q, we used the point charge model to estimate V_{zz}, the principal component of the EFG for the case of one first-neighbor oxygen vacancy because the results obtained with this simple model proved to be in excellent agreement in the case of cadmium impurities in indium sesquioxide[33] as well as in other compounds.[47] For $\lambda = 0.001$ ns^{-1}, $\nu = 2.2 \times 10^3$ ns^{-1}. In this way, ν results 10^4 times ω_Q and the correlation time, the time elapsed between jumps, $\tau_c \cong 5 \times 10^{-4}$ ns. These results justify the use of the Abragam and Pound approximation because our time window or time resolution is in the order of 1 ns.

In the case of the bimetallic catalysts, some Pt, a few percent probably, may be incorporated to the indium sesquioxide. If the oxidation state of Pt were 4+, they should be next to Cd. Point charge model calculations of the EFG show that the presence of Pt ions at first- or second-neighbor positions gave V_{zz} and then ω_Q values compatible with the frequency distributions δ shown in Tables 2 and 4 (see Table 6). Taking $\lambda = 0.007$ ns^{-1}, we obtain $\tau_c \cong 3.2 \times 10^{-3}$ ns. Under these considerations, our results show that the presence of Pt slows down the movement of the oxygen vacancies. In this way, and besides the limitations imposed for single temperature experiments, the fact that the addition of Pt causes an increase in the frequency jump of oxygen vacancies is a true conclusion, which derives from our experimental results. To obtain accurate quantitative information from this phenomenon, other experiments should be performed, probably with different techniques without the limitations PAC presents for this system at lower temperatures but with high sensitivity to local order (like XANES or EXAFS performed at In K-edge).

Accepting the validity of the simple model described above, our results show that the presence of Pt could not be detected through the hyperfine quadrupole frequencies, but its presence is revealed through the change in the relaxation process.

As said before, the presence of Pt is fundamental for the activation of the catalyst after reduction. When the monometallic catalyst In/FER is reduced, 60% of indium atoms end up as In_2O_3, whereas the rest form a new species not observed previously. Desimoni et al.[33] have found a similar distributed interaction when studying the oxidation of In in Ag. They have assigned this interaction to clusters of oxidized indium. They infer that these clusters, where the indium ions are 6-fold coordinated, are the origin of In_2O_3. Thus, no $(InO)^+$ phase remains in the catalysts. This explains its deactivation after the reduction treatment. In the case of the bimetallic catalyst, not only does the interaction corresponding to $(InO)^+$ at cationic exchange sites not disappear, but its population increases up to 100%. Some differences in the hyperfine parameters before and after reduction are found, which may be indicating that after reduction the fitted interaction corresponds to more than one site, and the increase in the population would be smaller.

Because of the high distribution δ there is no possibility of fitting two different sets of parameters for this interaction to clarify this point. This different behavior of the active phase after reduction for the two catalysts is difficult to validate based on our results. The disappearance of these sites in the monometallic catalyst can be understood assuming that Pt species block the zeolite channels during reduction, not allowing In atoms to migrate to the external surface. If this were the case, the increase of the third interaction in InPt/FER should not be explained as an increase in the active phase but because of the appearance of a new site, probably similar to the one found in In/FER after reoxidation. In this situation, the promoting effect should only be attributed to the presence of small metal clusters which may accelerate the velocity of the $NO + {}^1/_2O_2 \rightarrow NO_2$ reaction step and also the NO_2 adsorption capacity, thus increasing the overall reaction rate, as we have suggested before.[10] In the case of the ZSM5-based catalyst, the acidity strength could be a factor for these sites to remain. Regarding indium sesquioxide crystals, sintering processes are forming bigger crystals after reduction in FER based catalysts. This is possible because of the mobility of indium atoms during this process and in particular because of the mobility of those in the liquid phase.

Although the quantities of probes in liquid metallic indium in both FER samples are similar to those at cationic exchange sites before the reduction, the result found for In/ZSM5 makes us think that liquid indium is not produced from $(InO)^+$ at cationic exchange sites of the zeolite but from the total reduction of small indium sesquioxide crystallites. In effect, in the case of In/ZSM5, no liquid phase is present during reduction, although 46% of samples are at cationic exchange sites before the treatment. Moreover, as the fitted distributions δ of their interactions shown in Tables 1 and 3 indicate, indium sesquioxide crystallites are smaller in FER based catalysts than in In/ZSM5, what makes them easier to be reduced completely. In this way, liquid metallic indium forms from small crystallites that are completely reduced by hydrogen at 500 °C. No affirmation can be made regarding what happens with indium located at exchange sites during reduction, as it would not be reliable to fit a distribution and the relaxation at the same time in the spectra taken during H_2 treatments. The result found for In/FER after reduction makes us think that they disappear and reform in InPt/FER during reoxidation. The different behavior observed in this respect between In/FER and In/ZSM5 can be ascribed to the acidity of the support.

Conclusions

The relaxation of the hyperfine interactions observed by PAC during reduction treatments for the In/zeolite catalyst could be explained in terms of moving oxygen vacancies.

Platinum−indium interaction is observed for the first time in InPt/FER through the relaxation parameter measured by PAC. Nevertheless, this interaction seems not to be related to the promoting effect of Pt in the catalyst.

Small In_2O_3 crystals are apparently completely reduced by hydrogen at 500 °C, and liquid metallic indium or nanosized In_2O_3 crystallites with a null EFG are present in FER based catalysts. Larger crystals are not reduced.

Indium at exchange sites in the form of $(InO)^+$ species disappears after reduction in In/FER catalyst, and only indium sesquioxide and clusters of oxidized indium are observed after the treatment, explaining its deactivation after the reduction treatment.

The population of $(InO)^+$ exchanged at cationic sites of the zeolite in InPt/FER catalyst may be increased by as much as 100% after reduction. This could be one of the reasons for the promoting effect of Pt for the SCR of NO although other factors may also be responsible for this behavior.

Acknowledgment. The authors are grateful to Agencia de Promoción a la Investigación (Proj. 14-6971) and UNL (CAI+D '96 Program), Argentina. Thanks are also given to Jorge Runco for his technical assistance in the experimental PAC setup and to Elsa Grimaldi for the edition of the English manuscript.

References and Notes

(1) Frauenfelder, H.; Steffen, R. M. In *Alpha-, Beta- and Gamma-Ray Spectroscopy*; Siegbahn, K., Ed.; North-Holland: Amsterdam, 1968; Vol. 2, p 997.
(2) Lerf, A.; Butz, T. *Angew. Chem., Int. Ed. Engl.* **1987**, *26*, 110.
(3) Schatz, G.; Weidinger, A. *Nuclear Condensed Matter Physics: Nuclear Methods and Applications*, 2nd ed.; John Wiley & Sons Ltd: London, 1996; Chapter 5.
(4) Butz, T.; Lerf, A.; Vogdt, C.; Eid, A. M. M. *Hyperfine Interact.* **1983**, *15/16*, 915.
(5) Requejo, F. G.; Bibiloni, A. G. *Langmuir* **1996**, *12*, 2 (1), 51.
(6) Marchi, A. J.; Lede, E. J.; Requejo, F. G.; Rentería, M.; Irusta, S.; Lombardo, E. A.; Miró, E. E. *Catal. Lett.* **1997**, *48*, 47.
(7) Requejo, F. G.; Bibiloni, A. G.; Saitovich, H.; Silva, P. R. *J. Phys. Stat. Sol. (A)* **1990**, *120*, 105.
(8) Miró, E. E.; Gutierrez, L.; Ramallo López, J. M.; Requejo, F. G. *J. Catal.* **1999**, *188*, 375.
(9) Ramallo-López, J. M.; Requejo, F. G.; Gutierrez, L.; Miró, E. E., *Appl. Catal., B* **2001**, *29*, 35.
(10) Gutierrez, L. B.; Ramallo-López, J. M.; Irusta, S.; Miró, E. E.; Requejo, F. G. *J. Phys. Chem. B* **2001**, *105*, 9514.
(11) Ogura, M.; Hiramoto, S.; Kikuchi, E. *Chem. Lett.* **1995**, 1135.
(12) Meitzner, G.; Sinfelt, J. H. *Catal. Lett.* **1995**, *30*, 1.
(13) Bazin, D.; Mottet, C.; Tréglia, G. *Appl. Catal., A* **2000**, *200*, 47.
(14) Kikuchi, E.; Yogo, K. *Catal. Today* **1994**, *22*, 73.
(15) Klas, T.; Fink, R.; Krausch, G.; Platzer, R.; Voigt, J.; Wesche, R.; Schatz, G. *Surf. Sci.* **1989**, *216*, 270.
(16) Lindgren, B. *Europhys. Lett.* **1990**, *11*, 555.
(17) Butz, T.; Saibene, S.; Fraenzke, T.; Weber, M. *Nucl. Instrum. Methods Phys. Res. B* **1989**, *284*, 417.
(18) Mendoza-Zélis, L. A.; Bibiloni, A. G.; Caracoche, M. C.; López-García, A.; Martínez, J. A.; Mercader R. C.; Pasquevich, A. F. *Hyperfine Interact.* **1977**, *3*, 315.
(19) Bibiloni, A. G.; Desimoni, J.; Massolo, C. P.; Mendoza-Zélis, L. A.; Pasquevich, A. F.; Sánchez, F. H.; López-García, A. *Phys. Rev. B* **1984**, *29*, 1109.
(20) Massolo, C. P.; Desimoni, J.; Bibiloni, A. G.; Mendoza-Zélis, L. A.; Sánchez, F. H.; Pasquevich, A. F.; López-García, A. R. *Hyperfine Interact.* **1986**, *30*, 1.
(21) Elwenspoek, M.; Brinkmann, R.; v. Hartrott, M.; Kiehl, M.; Maxim, P.; Paulick, C. A.; Quitmann, D. *Hyperfine Interact.* **1983**, *15/16*, 577.
(22) Steffen R. M. *Adv. Phys.* **1955**, *4*, 294.
(23) Evenson, W. E.; McKale, A. G.; Su, H. T.; Gardner, J. A. *Hyperfine Interact.* **1990**, *61*, 1379.
(24) Baudry, A.; Boyler, P.; de Oliveira, A. L. *Phys. Lett.* **1980**, *79A*, 345.
(25) Marshall, A. G.; Meares, C. F. *J. Chem. Phys.* **1972**, *56*, 1226.
(26) Abragam, A.; Pound, R. V. *Phys. Rev. B* **1953**, *95*, 943.
(27) Baudry, A.; Boyer, P. *Hyperfine Interact.* **1987**, *35*, 803.
(28) Blume, M. *Phys. Rev.* **1968**, *174*, 351.
(29) Winkler, H.; Gerdau, E. *Z. Phys.* **1973**, *262*, 363.
(30) Evenson, W. E.; Gardner, J. A.; Wang, R.; Su, H. T.; McKale, A. G. *Hyperfine Interact.* **1990**, *62*, 283.
(31) Pál-Borbéli, P.; Beyer, H. K.; Kiyosumi, Y.; Mizukami, F. *Microporous Mesoporous Mater.* **1998**, *22*, 57.
(32) Ramallo-López, J. M.; Requejo, F. G.; Bibiloni, A. G.; Rentería, M.; Gutierrez, L.; Miró, E. E. *Z. Naturforsch.* **2000**, *55A*, 327.
(33) Desimoni, J.; Bibiloni, A.; Mendoza Zelis, L.; Pasquevich, A.; Sánchez, F.; López García, A. *Phys. Rev. B* **1983**, *28*, 5739.
(34) Feng, X.; Hall, W. K. *J. Catal.* **1997**, *166*, 368.
(35) Zhou, X.; Xu, Z.; Zhang, T.; Lin, L. *J. Mol. Catal. A: Chem.* **1997**, *122*, 125.
(36) Beyer, H.; Mihályi, R.; Minchev, Ch.; Neinska, Y.; Kanazirev, V. *Microporous Mater.* **1996**, *7*, 333.
(37) Dippel, M.; Maier, A.; Gimple, V.; Wider, H.; Evenson, W. E.; Rasera, R. L.; Schatz, G. *Phys. Rev. Lett.* **2001**, *87*, 95505.
(38) Oshima, Y.; Nangou, T.; Hirayama, H.; Takayanagi, K. *Surf. Sci.* **2001**, *476*, 107.
(39) Peng, X. S.; Wang, Y. W.; Zhang, J.; Wang, X. F.; Zhao, L. X.; Meng, G. W.; Zhang, L. D. *Appl. Phys. A* **2002**, *74*, 437.

(40) Murali, A.; Barve, A.; Leppert, V. J.; Risbud, S. H.; Kennedy, I. M.; Lee, H. W. H. *Nano Lett.* **2001**, *1*, 287.
(41) Elwenspoek, M.; Brinkmann, R.; v. Hartrott, M.; Kiehl, M.; Maxim, P.; Paulick, C. A.; Quitmann, D. *Hyperfine Interact.* **1983**, *15/16*, 577.
(42) Gardner, J. A.; Jaeger, H.; Su, H. T.; Haygarth, J. C. *Physica B* **1988**, *150*, 223.
(43) Su, H. T.; Wang, R.; Fuchs, H.; Gardner, J. A.; Evenson, W. E.; Sommers, J. A. *J. Am. Ceram. Soc.* **1990**, *73*, 3215.
(44) Wang, R.; Gardner, J. A.; Evenson, W. E.; Sommers, J. A. *Phys. Rev. B* **1993**, *47*, 638.
(45) Requejo, F. G.; Bibiloni, A. G.; Massolo, C. P.; Freitag, K. *Mod. Phys. Lett. B* **1994**, *8*, 329.
(46) Pryde, A. K. A.; Vyas, S.; Grimes, R. W.; Gardner, J. A.; Wang, R. *Phys. Rev. B* **1995**, *52*, 13214.
(47) Rentería, M.; Massolo, C. P.; Bibiloni, A. G. *Mod. Phys. Lett. B* **1992**, *6*, 1819.